PRACTICAL NUMERICAL SIMULATION METHOD FOR ESTIMATING LOCAL SCOURING AROUND A PIER ~ BOTTOM VELOCITY COMPUTATION METHOD BASED ON DEPTH INTEGRATED MODEL

T. Uchida[1] and S. Fukuoka[2]
1. Research and Development Initiative, Chuo University, 1-13-27 Kasuga, Bunkyo-ku, Tokyo, 112-8551, Japan, (utida@tamacc.chuo-u.ac.jp)
2. Research and Development Initiative, Chuo University, 1-13-27 Kasuga, Bunkyo-ku, Tokyo, 112-8551, Japan, (sfuku@tamacc.chuo-u.ac.jp)

ABSTRACT

In this paper, for estimating local scouring around a pier, the Bottom Velocity Computation (BVC) method is developed based on the depth integrated model. The governing equations of the BVC method are composed of depth-integrated horizontal vorticity and water surface velocity equations in addition to shallow water equations and a depth averaged turbulence energy transport equation. To compute bed variation, non-equilibrium bed load equation is proposed. The adequacy of the model is discussed through the comparisons with the laboratory experimental results for flows and bed variations around a pier. The pier scour is induced mainly by the horseshoe vortex. The horseshoe vortex with radial diverging bed-surface flow from the top of the pier is produced by the extension and rotation of the horizontal vortex filament in approaching flow. On the other hand, bed-surface flow converges and deposits sediment downstream of the pier. This paper shows that these important flow characteristics around a pier are reproduced by the BVC method. And computed scour hole around a pier is similar to that of the measurement. The above indicates the BVC method with the bed variation analysis by non-equilibrium sediment transport model is useful to simulate the severe local scour in front of structures.

1. INTRODUCTION

River engineers are faced with urgent task of checking the safety degree against floods, because the safety level of rivers in Japan is predicted to be reduced by the global warming. A numerical model for bed variations in rivers during floods is required to assess the risk of river structures due to local scouring.

Local scour around a pier has attracted a lot of interest from engineers and researchers for a long time. Recently, the horseshoe vortex and local scour around a pier have been calculated successfully by full 3D turbulence models coupled with sediment transport models (Olsen & Melaaen, 1993; Olsen & Kjellesvig, 1998; Nagata et al., 2005; Roulund et al., 2005). However, full 3D turbulence models are still limited for application to floods and bed variations in natural rivers. So, a practical and reliable model for flows and bed variations during floods are highly required.

Depth integrated models have been used for computations of flood flows and bed variations in rivers (Fukuoka, 2005; Wu, 2008). A 2D model based on the shallow water equations does not give sufficient accuracy in calculating local scouring around outer bank in curved channels, contracting sections, river confluences, and river structures. For such conditions, bottom velocity (velocity near bed surface) which determines sediment motions is different from that for uniform flow, as shown in Figure 1. For this reason, many improved depth integrated models have been developed, especially for a helical flow in a curved or meandering channel. Those include full-developed secondary flow model without considering effects of secondary flow on vertical distribution of stream-wise velocity (e.g. Engelund, F., 1974; Nishimoto et al., 1992), refined secondary flow models with non-equilibrium (e.g. Ikeda & Nishimura, 1986; Finnie et al., 1999) and mean flow redistribution effects (e.g. Blanckaert & de Vriend, 2003). As more versatile method for evaluating vertical velocity distributions, a quasi-3D model, in which equations for vertical velocity distribution are computed, has been developed (e.g.

Ishikawa et al., 1986; Fukuoka et al., 1992; Jin & Steffler, 1993; Yeh & Kennedy, 1993). The above mentioned models are categorized in the efficiently-simplified 3D model with the assumption of hydrostatic pressure distribution for each objective of the computation, as shown in Figure 2. However, it is known that these models are still-inadequate for local scouring induced by complex flows around a pier, because they cannot consider effects of flows due to non-hydrostatic pressure distribution on vertical velocity distributions.

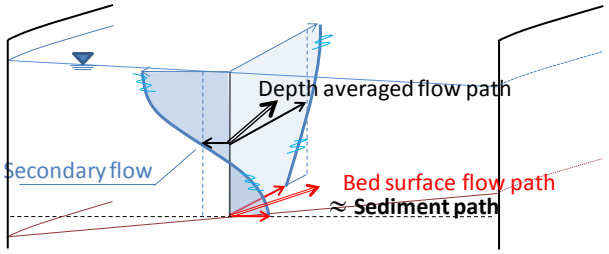

Figure 1 **Helical flow due to the centrifugal force in curved channels**

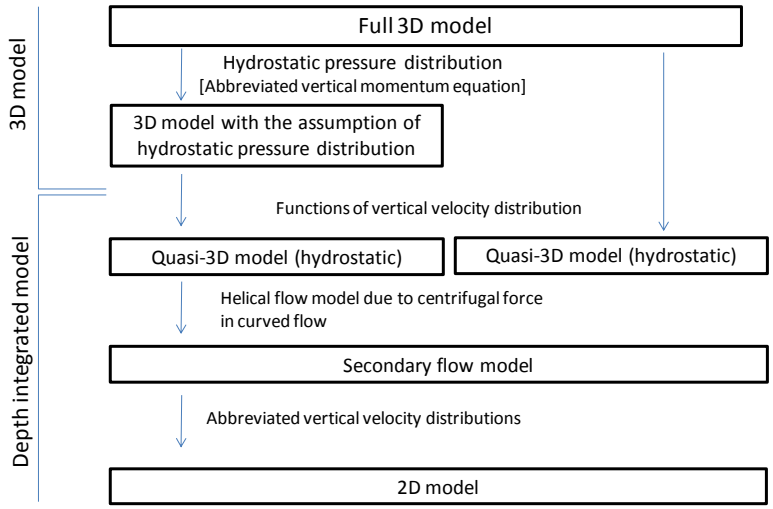

Figure 2 **Categorization of depth integrated models by derivations**

Ghamry & Steffler (2002) proposed quasi-3D model with non-hydrostatic pressure distribution based on moment equations. However, the model capability for complex flow fields around structures is remain incompletely understood. Recently, we had developed a new depth integrated model without the assumption of the vertical pressure distribution, in which shallow water equations and horizontal vorticity equations are solved to compute vertical velocity distributions. It was demonstrated that the model can simulate complex flow fields induced by a tributary entry (Uchida & Fukuoka, 2009). In this paper, for estimating local scouring around a pier, the Bottom Velocity Computation (BVC) method is developed based on the depth integrated model (Uchida & Fukuoka, 2009). To compute bed variation, non-equilibrium bed load equation is proposed and combined with the BVC method. And the adequacy of the model is discussed through the comparisons with the laboratory experimental results for flows and bed variations around a pier.

2. BOTTOM VELOCITY COMPUTATION METHOD

2.1 Basic concept

Figure 3 shows Bottom Velocity Computation (BVC) method. We define the bottom z_b as the surface on the shin vortex layer δz_b on the bed, as shown in Figure 3. The velocity on the bottom u_{bx} is computed by the BVC method. With Stokes' theorem, velocity difference δu_x between water surface u_{sx} and bottom surface u_{bx} is represented by depth-integrated vorticity $\Omega_y h$ and spatial difference of depth-integrated vertical velocity Wh. The non-dimensional form is :

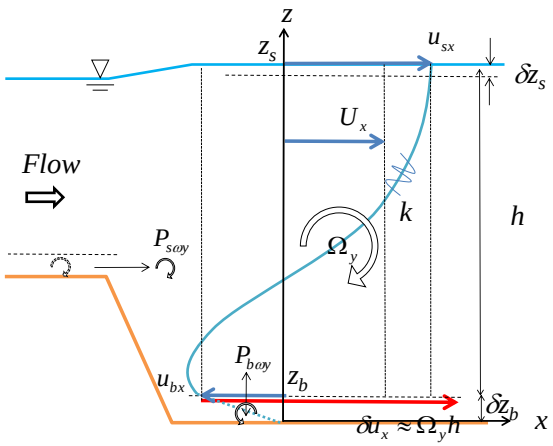

Figure 3 The concept of Bottom Velocity Computation Method

$$\delta u^*_x = \Omega^*_y h^* + \left(h_0 / L_0\right)^2 \partial W^* h^* / \partial x^* \tag{1}$$

where, $\Omega^*_y = \Omega_y h/U_0$, $h^*=h/h_0$, $x^*=x/L_0$, $\delta u^*_x = \delta u_x/U_0$, $W^*=W/W_0=Wh_0/U_0L_0$, h_0: representative water depth (vertical scale of flow), L_0: horizontal scale of flow, U_0: representative horizontal velocity, W_0: representative vertical velocity. For shallow water flow, the second term is neglected. That means, for many flow fields in river, we can evaluate the bottom velocity u_{bx} by water surface velocity u_{sx} and depth-integrated horizontal vorticity $\Omega_y h$.

The governing equations of the BVC method are composed of depth-integrated horizontal vorticity and water surface velocity equations in addition to shallow water equations and a depth averaged turbulence energy transport equation. The important advantage of the BVC method is the ability to compute bottom velocity distribution of the complex flow field around the river structure due to non-hydrostatic pressure distribution. The local scouring around the structure is calculated by using the bottom velocity with continuity equation for sediment and non-equilibrium sediment transport equations.

2.2 Vertical velocity distribution and governing equations

- Vertical velocity distribution and bed shear stress

Velocity distributions above very thin vortex layer on bed are computed in the BVC method. The Polynomial equation of vertical velocity distribution is assumed. Then, by using depth averaged velocity U_i, velocity difference δu_i between water surface and bed surface, water surface velocity u_{si}, and no vertical velocity gradients on water surface, the vertical velocity distribution of a cubic curve is obtained:

$$u_i = U_i + \Delta u_i\left(12\eta^3 - 12\eta^2 + 1\right) - \delta u_i\left(4\eta^3 - 3\eta^2\right) \tag{2}$$

where, $\Delta u_i = u_{si} - U_i$, $\delta u_i = u_{si} - u_{bi}$, $\eta = (z_s - z)/h$, z_s: water level, h: water depth. The uniform velocity distribution is derived by equilibrium water surface velocity $u_{sei} = (U_i + \delta u_i - \Delta u_i)/2$ and equilibrium velocity difference δu_{ei}. For the equilibrium condition, shear stress τ_{zi} is written as:

$$\tau_{zi} = \tau_{bi}\eta = \nu \frac{du_i}{dz}\eta = \frac{2\nu\delta u_i}{h}\eta \tag{3}$$

where, $\tau_{bi} = i$ direction bed shear stress defined as:

$$\tau_{bi} = C_0^{\,2} U_i U = c_b^{\,2} u_{bi} u_b \tag{4}$$

where, $U^2 = U_i U_i$, $u_b^{\,2} = u_{bi} u_{bi}$. δu_i for the equilibrium condition is given by:

$$\delta u_i = C_0^{\,2} U_i U \frac{h}{2\nu} = c_b^{\,2} u_{bi} u_b \frac{h}{2\nu} \tag{5}$$

With the depth averaged eddy-viscosity $\nu = \alpha u_* h$, $\alpha = \kappa/6$, the relationship between c_b and C_0 is described as:

$$c_b = C_0 / \left(1 - 2C_0/\kappa\right) \tag{6}$$

C_0 is described by manning roughness coefficient, $C_0^{\,2} = gn^2/h^{1/3}$.

- Water surface velocity

The equations for the water surface velocities are derived by assuming very thin layer just below water surface δz_s (see Figure 3), neglecting water surface curvature:

$$\frac{\partial u_{si}}{\partial t} + u_{sj}\frac{\partial u_{si}}{\partial x_j} = -g\frac{\partial z_s}{\partial x_i} + P_{si} \tag{7}$$

where, P_{si}, shearstress acting on δz_s, is represented by Equation (8).

$$P_{si} = \frac{2\nu_t}{h^2}\left\{12C_{ps}\left(u_{sei} - u_{si}\right) - 3\delta u_i + 6\Delta u_i\right\} \tag{8}$$

where, C_{ps}=3.

- Depth averaged horizontal velocity and water depth

Equations for water depth h and depth averaged velocity vectors U_i (shallow water equations) with occupancy ratio of water λ described as:

$$\frac{\partial \lambda h}{\partial t} + \frac{\partial U_j \cdot \lambda h}{\partial x_j} = 0 \tag{9}$$

$$\frac{\partial \lambda U_i h}{\lambda h \partial t} + \frac{\partial \lambda U_i U_j h}{\lambda h \partial x_j} = -g\frac{\partial z_s}{\partial x_i} - \frac{\tau_{0i}}{h} - \frac{\tau_{swi}}{R_{sw}} + \frac{\partial \lambda h \tau_{ij}}{\lambda h \partial x_j} \tag{10}$$

where, τ_{swi} =shear stress acting on side wall, R_{sw}=hydraulic radius of side wall. τ_{ij} is horizontal shear stress:

$$\tau_{ij} = 2\nu_t S_{ij} - \overline{u_i' u_j'} - 2/3 \cdot \delta_{ij} \cdot k \tag{11}$$

where, k=depth averaged turbulence energy, S_{ij}=strain ratio tensor of depth averaged velocity vectors U_i. The second term is produced by vertical velocity distribution, which is defined as:

$$\overline{u_i' u_j'} = \frac{13\Delta u_i \Delta u_j - 2\Delta u_i \delta u_j - 2\delta u_j \Delta u_i + 3\delta u_i \delta u_j}{35} \tag{12}$$

k is computed by Eq.(13), which is known as one-equation model:

$$\frac{\partial k}{\partial t} + U_j \frac{\partial k}{\partial x_j} = \frac{1}{h\lambda} \frac{\partial}{\partial x_i} \left(\frac{\nu h \lambda}{\sigma_k} \frac{\partial k}{\partial x_i} \right) + \frac{D_{sw}}{R_{sw}} + P_k - \varepsilon \tag{13}$$

where, $\nu = C_\mu k^2/\varepsilon$, $\varepsilon = C_\varepsilon k^{3/2}/\Delta$, C_μ=0.09, $C_\varepsilon/\Delta = 1.7/h$ (Nadaoka & Yagi, 1998). With using vertical velocity distribution (2), the production term P_k is derived as:

$$\frac{P_k}{\nu_t} = 2\left(S^2 + \frac{13}{35}\Delta S^2 - \frac{4}{35}\Delta S_{ij}\delta S_{ij} + \frac{3}{35}\delta S^2 \right) + \frac{4C_h}{5h^2}\left(8\Delta u^2 - 7\Delta u_i \delta u_i + 2\delta u^2 \right) \tag{14}$$

where, $S^2 = S_{ij}S_{ij}$, $\Delta S^2 = \Delta S_{ij}\Delta S_{ij}$, $\delta S^2 = \delta S_{ij}\delta S_{ij}$, $\Delta u^2 = \Delta u_i \Delta u_i$, $\delta u^2 = \delta u_i \delta u_i$, δS_{ij}=strain ratio tensor of δu_i, ΔS_{ij}=strain ratio tensor of Δu_i. $C_h = 9(\alpha C_\varepsilon)^4/C_\mu^3$, $\alpha = \nu_{te}/u_* h = \kappa/6$, ν_{te}: equilibrium depth averaged kinematic eddy viscosity. The model is equivalent of zero-equation model for the equilibrium condition of k. And in this model, the last term of equation (11) is eliminated, because the normal stress is assumed as hydrostatic pressure distribution.

- Depth integrated horizontal vorticity equations

The velocity difference δu_i is computed by using depth integrated vorticity for shallow water conditions, as discussed above:

$$\delta u_i = \varepsilon_{ij3} \Omega_j h \tag{15}$$

where, ε_{ij}^3=permutation symbol ($\varepsilon_{123} = -\varepsilon_{213} = 1$, $\varepsilon_{113} = \varepsilon_{223} = 0$), Ω_i =depth averaged vorticity vectors. The equation for Ω_i is described by:

$$\frac{\partial \Omega_i h}{\partial t} = ER_{\sigma i} + P_{\omega i} + \frac{\partial h D_{\omega ij}}{\partial x_j} \tag{16}$$

where,

$$ER_{\sigma i} = u_{si}\omega_{s\sigma} - u_{bi}\omega_{b\sigma},\ D_{\omega ij} = -U_j\Omega_i + U_i\Omega_j + \overline{\omega_j' u_i'} - \overline{\omega_i' u_j'} + \frac{\nu_t}{\sigma_\omega}\frac{\partial \Omega_i}{\partial x_j},$$

$$\overline{\omega_i' u_j'} = \frac{6}{5}\Delta\omega_i \delta u_j - \Omega_i\left(\frac{\delta u_j}{2} + \frac{\Delta u_j}{5} \right), \quad \Delta\omega_i = -\varepsilon_{ij3}\Delta u_j / h$$

2.3 Bottom vorticity and production of vorticity from vortex layer

The production term $P_{\omega i}$ of the vorticity equation (16) represents net vorticity flux from the thin vortex layer on bed. For flat bed condition, the flux is induced by the turbulent mixing ($P_{b\omega i}$). In addition, the flux is supplied by the separation downstream of the abrupt change of bed slope ($P_{s\omega i}$), as shown in Figure 3. The production term is defined as the sum:

$$P_{\omega i} = P_{b\omega i} + P_{s\omega i} \tag{17}$$

$P_{b\omega i}$ is approximated by the product of the kinematic eddy viscosity and the vertical gradient of vorticity near the bed:

$$P_{b\omega i} = C_{p\omega} \nu_{tb} \frac{\omega_{bei} - \omega_{bi}}{h} \tag{18}$$

where, $C_{p\omega}=3\kappa/\alpha$, ν_{tb}: equivalent depth averaged value of bottom kinematic eddy viscosity, $\nu_{tb}=\max(\alpha^2 h^2 \omega_b,\ \alpha^2 h^2 \omega_{be},\ \nu_t)$, $\omega_b{}^2=\omega_{bi}\omega_{bi}$, $\omega_{be}{}^2=\omega_{bei}$, ν_t: depth averaged kinematic eddy viscosity, ω_{bi}: bottom vorticity, ω_{bei}: equilibrium bottom vorticity for bottom velocity u_{bi}, $\omega_{bei}=-\varepsilon_{ij3}c_b u_{bi}/\alpha h$, ω_b: bottom vorticity. The bottom vorticity is defined by Equation (19), minimizing the production term between $\omega_{bi}=\omega_{bci}$ and $\omega_{bi}=\omega_{bqi}$:

$$\begin{cases} \Delta\omega_{bci}\Delta\omega_{bqi} < 0: & \omega_{bi} = \omega_{bei} \\ \Delta\omega_{bci}\Delta\omega_{bqi} > 0: & \begin{cases} |\Delta\omega_{bci}| < |\Delta\omega_{bqi}|: & \omega_{bi} = \omega_{bci} \\ |\Delta\omega_{bci}| > |\Delta\omega_{bqi}|: & \omega_{bi} = \omega_{bqi} \end{cases} \end{cases} \tag{19}$$

where, $\Delta\omega_{bci}=\omega_{bei}-\omega_{bci}$, $\Delta\omega_{bqi}=\omega_{bei}-\omega_{bqi}$, $\omega_{bci}=6(\delta u_i-12\Delta u_i)/h$, $\omega_{bqi}=2\Omega_i$.

The flux supplied by the separation $P_{s\omega i}$ is represented by the product of the bottom layer integrated vorticity and the bottom layer averaged velocity:

$$P_{s\omega x}\Delta x = \begin{cases} |u_{by}/2|\cdot(-u_{by}) & (\delta z_y > \tan\phi) \\ 0 & (\delta z_y < \tan\phi) \end{cases}, \quad P_{s\omega y}\Delta y = \begin{cases} |u_{bx}/2|\cdot(+u_{bx}) & (\delta z_x > \tan\phi) \\ 0 & (\delta z_x < \tan\phi) \end{cases} \tag{20}$$

where, Δx, Δy: computational grid size of x, y direction, $\delta z_x=z_{xx}\Delta x$, $\delta z_y=z_{yy}\Delta y$, z_{xx}, z_{yy}: second order differential of bed level computational by x, y.

2.4 Numerical schemes

The explicit conservative CIP scheme for shallow water flows (Uchida, 2006) is adopted for computations of water depth and depth averaged velocity vectors. In the model, to directly capture the effect of distributed parameters in the Cartesian coordinate system, each control volume ij has three kinds of variables, i.e., the value at the intersection of the grid (Point Value), the averaged value along the side of the grid (Line-averaged Value) and the averaged value over the grid (Area-averaged Value). Those values are computed all together based on CIP-CSL scheme (Nakamura et al., 2001). All the variables in the governing equations are set on the same location. The utilization of multi-valuables on a computational cell enables us to capture complex geometry even on the Cartesian coordinate system. The above scheme is not adopted for computations of the equations for water surface velocity, the depth averaged turbulence energy and vorticity. Those averaged value of the computational cell are computed by traditional scheme.

3. COMPUTATIONAL METHOD FOR BED VARIATION

3.1 Continuity equation and momentum equation for sediment

The time variation of bed topography is computed by the continuity equation for sediment:

$$(1-\lambda_B)\frac{\partial z}{\partial t} + \frac{\partial q_{Bi}}{\partial x_i} = 0 \tag{21}$$

where, λ_B: sediment porosity, q_{Bi}: bedload sediment transport rate. The equation for the bedload rate is derived by momentum equation for sediment:

$$\frac{\partial q_{Bi}}{\partial t}+\frac{\partial u_{Bj}q_{Bi}}{\partial x_j}=\left(Pu_{BPi}-Du_{BDi}\right)+m_* h_B\left(\gamma_{ei}-\gamma_i\right) \tag{22}$$

where, u_{Bi}: sediment particle velocity of bedload, Pu_{BPi}: gain momentum from bed material, Du_{BDi}: loss momentum by particle deposition, $m_*=\mu_k sg\cos\theta/(s+1+C_M)$, C_M : coefficient of added mass, μ_k: dynamic friction coefficient of sediment, s: specific gravity of sediment in water, θ: maximum grade of bed, $h_B=q_B/u_B$, $q_B=q_{Bi}q_{Bi}$, $u_B=u_{Bi}u_{Bi}$, γ_i, γ_{ei}: i component of unit vector of sediment movement and its equilibrium value. u_B, u_{Be}, h_B are given by reference to Ashida & Michiue (1974).

The first term in right side for momentum exchange between bed load and bed materials is described as:

$$Pu_{BPi}-Du_{BDi}=q_{Be}u_{Bei}/L_e-q_B u_{Bi}/L \tag{23}$$

where, q_{Be}: equilibrium sediment transport rate of bed load, L, L_e: average particle step length and that for equilibrium condition. The step length formulae are assumed by reference to Phillips & Sutherland (1989). The second term in right side is derived by forces acting on sediment particles.

3.2 Bed tractive force and equilibrium bed load

The total resistance of bed is evaluated as bed shear stress of equation (3) in the present model. The total resistance of bed with sand waves is divided into form drag acting on sand waves and surface resistance acting on sediment particles. The latter is considered as bed tractive force which induces bed load (Ashida & Michiue, 1974). Generally, the surface resistance is evaluated by:

$$\tau_{bse}=(c_{bs}u_b)^2 \tag{23}$$

where, $1/c_{bs}=A_r+(1/\kappa)\ln(z_b/k_s)$, $A_r=8.5$, k_s: equivalent roughness. However, the above is assumed as a uniform flow condition and inadvisable in flow conditions around structures with local scouring. In this study, the surface resistance is evaluated by the Boussinesq approximation near bed to evaluate non-equilibrium flow conditions:

$$\tau_{bs}=c_v\nu_{tb}\left(\frac{\partial u}{\partial z}\right)_b=\frac{\nu_{tb}}{\nu_{te}}\left\{c_v\nu_{te}\cdot\left(\frac{\partial u}{\partial z}\right)_b\right\}=\frac{\nu_{tb}c_{bs}u_b}{\alpha h} \tag{24}$$

where, $c_v\nu_{tb}$: bottom kinematic eddy viscosity, ν_{te}: equilibrium depth averaged kinematic eddy viscosity. The bed tractive force and the critical shear stress of sediment particle on bed slope are given by Fukuoka & Yamasaka (1983). The equilibrium bed load is given by Ashida & Michiue (1974). And where the local bed slope exceeds the repose angle, the sand slide occurs in the model.

4. APPLICATION TO LOCAL SCOURING AROUND A PIER

4.1 Experimental and computational conditions

The present model is applied to the experiment for local scour around a pier by Fukuoka et al. (1997) to validate the model performance. Experiments were conducted in the channel with 27.5 m long, 1.5 m width, 1/600 initial bed slope and uniform sand material d=0.80 mm. A pier with 0.20 m diameter was installed at the center of the cross section in the channel. The experimental discharge was 0.066 m^3/s, and sediment supply rate at the upstream end was 8.8 cm^3/s. The average water depth h_0 and Fr number of the experiment were h_0=11.6 cm and Fr=0.4, respectively.

The computational domain includes the overall channel width from 5m upstream to 6m downstream of the pier. From about 2.5m upstream to about 4m downstream of the pier, uniform grid of dx=dy=0.025m is used, as shown in Figure 4. The experimental discharge and sediment supply rate are given at the upstream end of the domain and the fixed water level is given at the downstream end.

The downstream end water level and manning roughness n of channel bed are decided to adjust longitudinal water surface profiles between computation and measurement. And the equivalent roughness for bed tractive force is given by $k_s=2d$. The initial flow condition of the bed variation analysis is given by computation results for fixed flat bed with $z=0$ at the pier center section with initial bed slope 1/600.

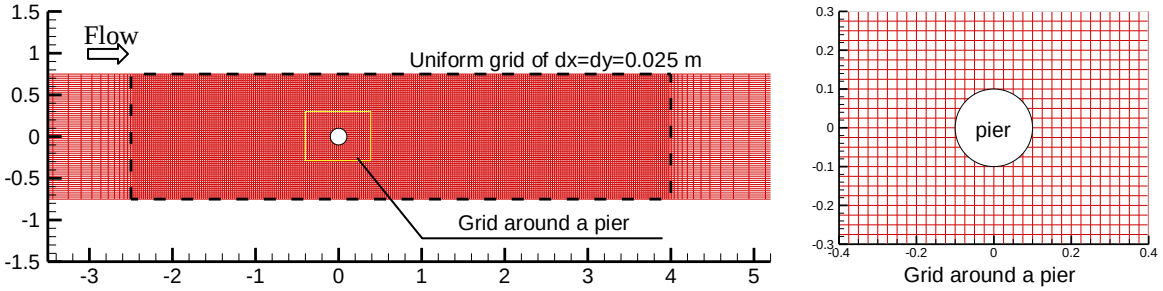

Figure 4 The computational domain and grid

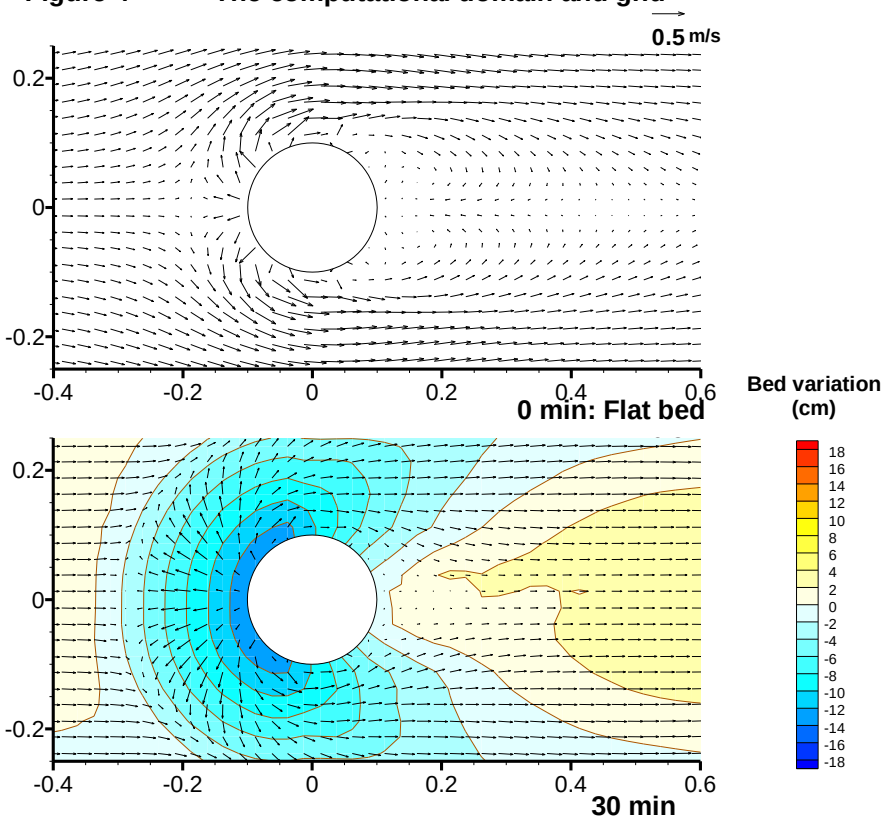

Figure 5 The computed bottom velocity fields on flat bed and scour bed after 30min.

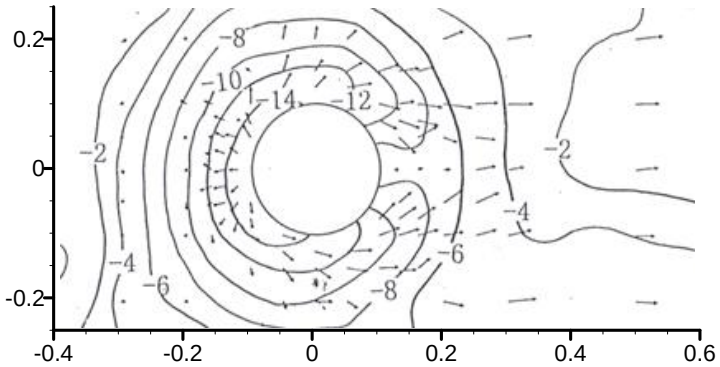

Figure 6 The measured bottom velocity fields for equilibrium stage (65 hours) (Fukuoka et al., 1997)

4.2 Computed results and discussion

Figure 5 shows computed temporally averaged bottom velocity fields on initial flat bed and computed local scour after 30 minutes. Figure 6 shows the measured bottom velocity field around the pier for the equilibrium condition (after 65 hours). In the experimental results, it is fined that radial bottom flows from the top of the pier induces local scour and the bottom flow runs around to the back of the pier with sediment deposition. These important characteristics of the bottom velocity around the pier are shown in the present model, especially for the radial bottom flow induced by the horseshoe vortex. The radial bottom flow after 30 minutes by the present model is developed from that on initial flat bed due to bed scouring. This phenomenon is similar as examined in previous experimental results by Melville & Raudkivi (1977) and computed results by the full 3D turbulence model (Nagata et al., 2005). As indicated above, the present model is reasonable to evaluate the bottom velocity fields around the pier, because the horseshoe vortex is mainly developed by the extension and rotation of the transverse vorticity in approaching flow.

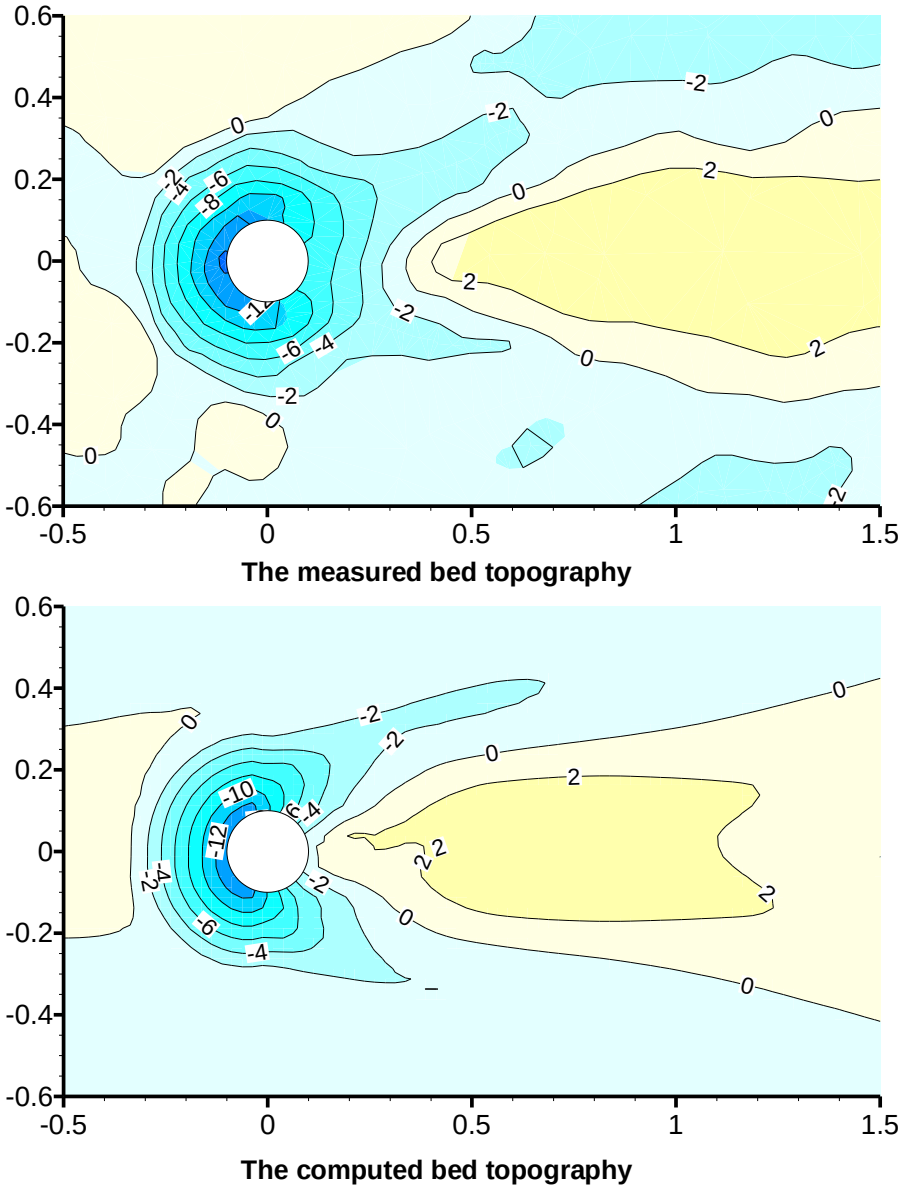

Figure 7 The comparison of between measured (Fukuoka et al., 1997) and computed bed topographies around the pier after 30 minutes

Figure 7 shows the comparison of bed topographies around the pier between measured (Fukuoka et al., 1997) and computed results after 30minutes. And Figure 8 shows the comparisons of longitudinal

and transverse bed profiles along the center-line of the pier. At the back of the pier, computed scour is not developed but computed sediment deposition is developed compared with those of the measurement. Roulund et al. (2005) also indicated that the scour depth at the back of the pier by the full 3D turbulence model with the bed variation model by the bed load sediment transport was smaller than that of the experiment. To improve this issue, a suspended load sediment transport model is required, as indicated by Roulund et al. (2005). However, in the upstream part of the pier, computed scour hole is similar to that of the measurement. And the upstream and lateral bed profiles of scour hole of the computation are in good agreement with those of the experiment. As indicated above, the present model is useful to simulate local scour in front of structures due to horseshoe vortex.

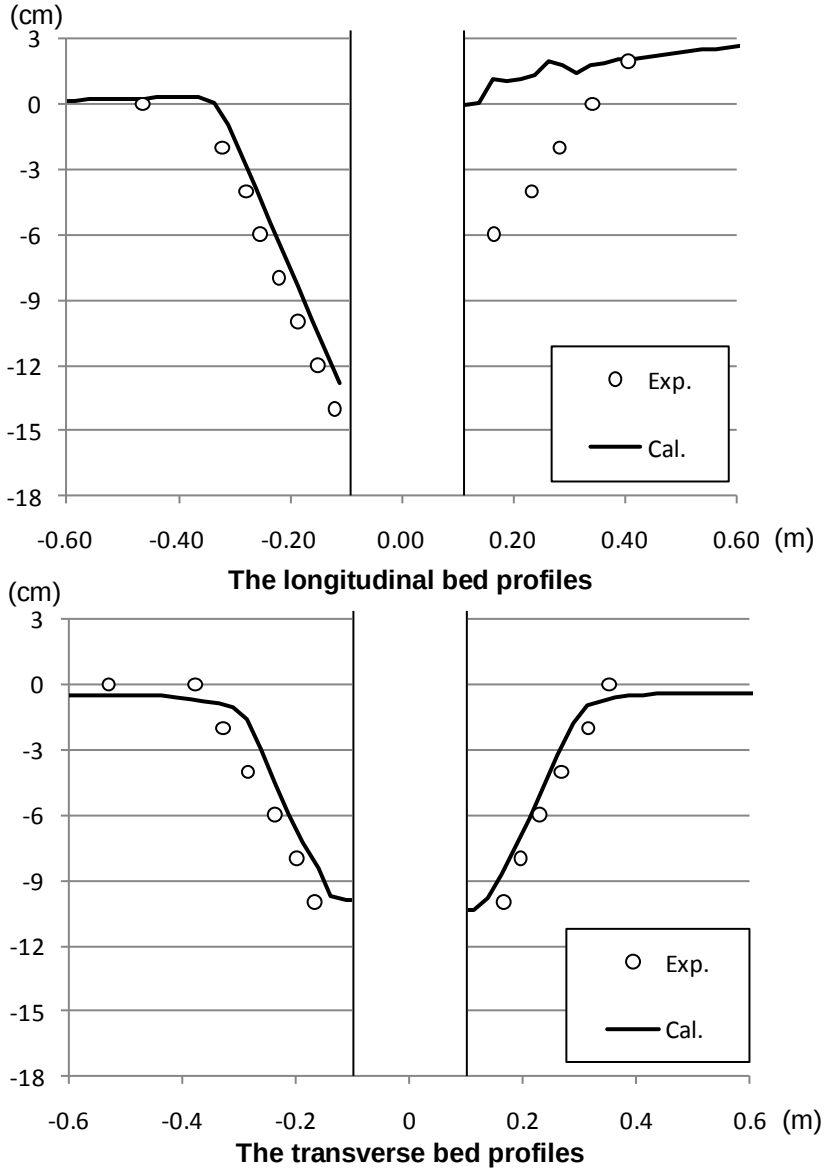

Figure 8 The comparison of bed between measured (Fukuoka et al., 1997) and computed bed profiles

5. CONCLUSIONS

This paper indicates that the bottom velocity is evaluated by water surface velocity and depth-integrated horizontal vorticity for shallow water flows. Based on this consideration, this study proposes a bottom velocity computation (BVC) method, in which depth-integrated horizontal vorticity and water surface velocity equations are solved in addition to shallow water equations and a depth averaged

turbulence energy transport equation. To develop a bed variation model for local scour around structures, non-equilibrium bed load equation is derived based on the momentum equation of the particle in the bed load sediment. It is demonstrated that the model can reproduce bottom velocity fields around the pier and the scour hole induced by the horseshoe vortex.

6. REFERENCES

Ashida, K. and Michiue, M.(1972). Study on hydraulic resistance and bed-load transport rate in alluvial stream. *Proceedings of the Japan Society of Civil Engineers*, Vol.206, pp.59-69, in Japanese.

Blanckaert, K. and de Vriend, H. J.(2003). Nonlinear modeling of mean flow redistribution in curved open channels. *Water Resources Research*, Vol.39, No.12, 1375, doi:10.1029/2003WR002068.

Engelund, F.(1974). Flow and bed topography in channel bends. *Journal of hydraulics division*, Proc. of ASCE, Vol.100, HY11, pp.1631-1648.

Finnie, J., Donnell, B., Letter, J., and Bernard, R.S.(1999). Secondary flow correction for depth-averaged flow calculations. *Journal of Engineering Mechanics*, ASCE, Vol.125, No.7, pp.848-863.

Fukuoka, S.(2005). Flood hydraulics and channel design. Morikita, Japan, in Japanese.

Fukuoka, S. and Yamasaka, M.(1983). Alternating bars in a straight channel. *Proceedings of the Japanese Conference on Hydraulics*, JSCE, pp.703-708, in Japanese.

Fukuoka, S., Miyagawa, T. and Toboishi, M.(1997). Measurements of flow and bed geometry around A cylindrical pier and calculation of its fluid forces. *Annual journal of hydraulic engineering*, JSCE, pp.729-734, in Japanese.

Ghamry, H. K. and Steffler, P.M.(2002). Two dimensional vertically averaged and moment equations for rapidly varied flows. *Journal of hydraulic research*, Vol.40, No.5, pp.579-587.

Ikeda, S. and Nishimura, T. (1986). Three-dimensional flow and bed topography in sand-silt meandering rivers. *Proceedings of the Japan Society of Civil Engineers*, Vol.369/II-5, pp.99-108, in Japanese.

Ishikawa, T., Suzuki, K. and Tanaka, M. (1986). Efficient numerical analysis of an open channel flow with secondary circulations. *Proceedings of the Japan Society of Civil Engineers*, Vol.375/II-6, pp.181-189, in Japanese.

Jin Y.-C. and Steffler, P.M.(1993). Predicting flow in curved open channels by depth-averaged method. *Journal of Hydraulic Engineering*, ASCE, Vol.119, No.1, pp.109-124.

Melville, B. W. and Raudkivi, A. J. (1977) Flow characteristics in local scour at bridge piers, *Journal of Hydraulic Research*, 15(4), 373-380.

Nagata, N., Hosoda, T., Nakato, T. and Muramoto, Y.(2005). Three-dimensional numerical model for flow and bed deformation around river structures. *Journal of Hydraulic Engineering*, ASCE, No.131, No.12, pp.1074-1087.

Nadaoka, K. and Yagi, H.(1998). Shallow-water turbulence modelling and horizontal large-eddy computation of river flow. *Journal of Hydraulic Engineering*, Vol.124, No.5, pp.493-500.

Nakamura, T., Tanaka, R., Yabe, T., and Takizawa, K. (2001). Exactly conservative semi-Lagrangian scheme for multi-dimensional hyperbolic equations with directional splitting technique. *Journal of Computational Physics* 174, pp. 171–207.

Nishimoto, N., Shimizu, Y. and Aoki, K. (1992). Numerical simulation of bed variation considering the curvature of stream line in a meandering channel. *Proceedings of the Japan Society of Civil Engineers*, Vol.456/II-21, pp.11-20, in Japanese.

Olsen, N. R. B. and Melaaen, M. C. (1993). Three-dimensional numerical calculation of scour around cylinders. *Journal of Hydraulic Engineering*, ASCE, No.119, No.9, pp.1048-1054.

Olsen, N. R. B. and Kjellesvig, H. M. (1998). Three dimensional numerical flow modeling for estimation of maximum local scour depth. *Journal of Hydraulic Research*, IAHR, 36(4), pp.579-590.

Phillips, B.C. and Sutherland, A.J. (1989). Spatial lag effects in bed load sediment transport, *Journal of Hydraulic Research*, Vol.27, No.1, pp.115-133.

Roulund, A., Sumer, B.M., Fredsøe, J. and Michelsen, J. (2005). Numerical and exparimantal investigation of flow and scour around a circular pile. *Journal of Fluid Mechanics*, 534, pp.351-401.

Uchida, T. (2006). A CIP-based method for shallow water flows in complex geometries using Cartesian grids. *Proceedings of 7th International Conference on Hydroscience and Engineering*, ICHE-2006.

Uchida, T. and Fukuoka, S. (2009). A depth integrated model for 3D turbulence flows using shallow water equations and horizontal vorticity equations. *33rd IAHR Congress*: *Water Engineering for a Sustainable Environment*, pp.1428-1435.

Yeh, K.-C. and Kennedy, J..F. (1993). Moment model of nonuniform channel-bend flow. I: fixed beds. *Journal of Hydraulic Engineering*, ASCE, Vol.119, No.7, pp.776-795.

Wu, W. (2008). Computational river dynamics, Taylor & Francis, London.